OPTICS, QUANTUM ELECTRONICS

Double Radiooptical Resonance in ^{87}Rb Atomic Vapor in Cells with Antirelaxation Wall Coating

A. N. Litvinov^a, G. A. Kazakov^b, B. G. Matisov^b, and I. E. Mazets^a

^{a} *Ioffe Physico-Technical Institute, Russian Academy of Sciences,*
Politekhnicheskaya ul. 26, St. Petersburg, 194021 Russia

e-mail: anprolvy@list.ru

^{b} *St. Petersburg State Polytechnical University, Politekhnicheskaya ul. 29, St. Petersburg, 195251 Russia*

e-mail: kazjor@rambler.ru

Received May 22, 2008

Abstract—The object of investigation is double radiooptic resonance in ^{87}Rb atomic vapor contained in a cell covered by an antirelaxation coating. The Dicke narrowing is studied in terms of the quantum-kinetic approach. It is found that optical pumping using a laser with a "wide" radiation spectrum makes it possible to improve the short-term stability of the frequency standard by an order of magnitude compared with a narrow-spectrum laser.

PACS numbers: 32.80.Bv, 06.30.Ft, 42.50.Gy

INTRODUCTION

Double radiooptical resonance (DROR) results from interaction of bichromatic radiation (a combination of resonance optical and microwave fields) with atoms. This effect is fundamental for designing magnetometers [1–4] and quantum frequency standards [4, 5]. Magnetometers are finding wide application in geological exploration [6], underwater prospecting, fundamental physics, etc. In recent years, the scope of their application has been considerably extended encroaching unconventional areas such as medicine. In 2007, specialists working at the National Institute of Standards and Technologies (United States) demonstrated an optical magnetometer with a room-temperature sensitivity of 70 fHz$^{-1/2}$ [7], which allows doctors, for example, to detect the magnetic fields of heart and brain [8] and thereby gain a much deeper insight into the functioning of these organs. Magnetometers can also be used in measuring weak fields in space, which is of crucial importance for exploring objects in near and deep space [9], predicting seismic activity [6], etc.

Quantum frequency standards are of no less significance, specifically, for developing navigation and positioning systems (such as GPS, GLONASS, and GALILEO) and telecommunications network synchronization systems, as well as for checking fundamental physical laws.

An important characteristic of any quantum discriminator is figure of merit Q, which depends on the amplitude and width of resonance. These parameters, in turn, depend on the time of coherent interaction between an atom and exciting fields. The main factor preventing the atom from being in coherence with the optical and microwave fields is its depolarization in collisions with cell walls.

Another problem is the Doppler broadening of the rf transition. This effect can be interpreted as the departure of a moving atom from a region where the field has a definite phase (this region is about microwave field wavelength λ across), which also cuts the time of atom–field coherent interaction. Thus, major difficulties encountered in improving the figure of merit are concerned with extension of this time.

There are two ways of extending the time of coherent interaction between an atom and exciting fields: letting a buffer gas in a cell with active atoms and using a cell with walls covered by an antirelaxation coating. When a buffer gas (a gas upon collisions with atoms or molecules of which almost all active atoms remain polarized) is introduced into the cell in a concentration exceeding the concentration of active atoms roughly by six orders of magnitudes, the free path of active atoms shortens drastically. Accordingly, their depolarization due to collisions with walls and the velocity of their displacement over a distance on the order of λ decrease considerably. However, this method suffers from a number of disadvantages, one of which is the shift and broadening of the frequency of the reference transition due to Pauli exchange repulsion and van der Waals attraction (which do not compensate for each other) arising when paramagnetic active atoms collide with diamagnetic atoms or molecules of the buffer gas.

More than 50 years ago, Robinson et al. [10] suggested another approach free of the above disadvantages. The basic idea here is to cover the walls of the cell by a special antirelaxation coating (usually paraf-

fin). In this case, the probability of atom depolarization due to collisions with the wall decreases considerably (by four orders of magnitude). It has been found recently that the relaxation coating ages fairly slowly (the frequency of the microwave transition shifts by less than 10 Hz for 30 years [1]). This finding disproves the earlier supposition that the antirelaxation coating has a short lifetime. The width of DROR studied in such cells was found to be 47 Hz [12]. In this work, we study DROR in ^{87}Rb atomic vapor contained in a laser-pumped buffer-gas-free cell with and without an antirelaxation coating on the walls. A theory of DROR developed here is based on quantum kinetic equations for the density matrix. The type of coating is embodied in boundary conditions. Unlike in [13], where DROR was considered in terms of a three-layer model, here the resonance is studied for a real ^{87}Rb atom with regard to the hyperfine and Zeeman structures of both ground and excited states.

1. QUANTUM KINETIC EQUATIONS FOR DROR

Consider interaction of a ^{87}Rb atom with optical (laser) and microwave fields. The atom is placed in permanent magnetic field **B** that removes degeneracy in projection of the total momentum of the atom onto a quantization axis given by the magnetic field. Levels participating in ^{87}Rb atom excitation can be split into two groups: levels of the $S_{1/2}$ ground state (g) and those of the excited $P_{1/2}$ or $P_{3/2}$ state (e). The former, in turn, can also be split into two groups (g_1 and g_2) corresponding to the hyperfine components of the ground state with total momenta $F_g = 1$ and 2, respectively (Fig. 1). The optical, **E**, and microwave, **H**, fields are given by

$$\mathbf{E}(\mathbf{r}, t) = \mathbf{E}_0 \exp[i(\mathbf{k} \cdot \mathbf{r} - \omega t)] + \text{c.c.}, \qquad (1)$$

$$\mathbf{H}(\mathbf{r}, t) = \mathbf{H}_0 \exp[i(\mathbf{q} \cdot \mathbf{r} - \omega_m t)] + \text{c.c.}, \qquad (2)$$

where $\mathbf{E}_0$ and $\mathbf{H}_0$ are the amplitudes of the respective fields, **k** and **q** are their wavevectors, and ω and ω_m are their frequencies. In (1) and (2), "c.c." means the complex conjugate.

To describe the interaction of the atoms with fields $\mathbf{E}(\mathbf{r}, t)$ and $\mathbf{H}(\mathbf{r}, t)$, we apply the apparatus of density matrix $\hat{\rho}(\mathbf{r}, \mathbf{p}, t)$ in the Wigner representation. The equations for density matrix elements ρ_{ij} in the case of the atomic system subjected to an external electromagnetic field have the form

$$\dot{\rho}_{ij}(\mathbf{r}, \mathbf{p}, t) \equiv \frac{\partial \rho_{ij}}{\partial t} + \frac{\mathbf{p}}{m} \cdot \nabla \rho_{ij}$$

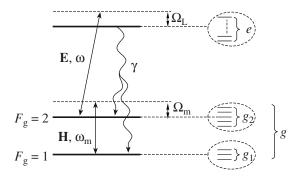$$= -\frac{i}{\hbar} \sum_k [H_{ik}\rho_{kj} - \rho_{ik}H_{kj}] + (\hat{\hat{\Gamma}}\hat{\rho})_{ij}, \qquad (3)$$

Fig. 1. Excitation of the ^{87}Rb atom. Ω_L and Ω_m are the detunings of the optical and microwave fields, respectively, and γ is the rate of excited state spontaneous decay.

where H_{ik} and H_{kj} are the elements of Hamiltonian $\hat{H}$, $\hat{\hat{\Gamma}}$ is the relaxation operator, and m is the atomic mass. Hamiltonian $\hat{H}$ can be represented as

$$\hat{H} = \hat{H}_0 + \hbar\hat{V}, \qquad (4)$$

where $\hat{H}_0$ is the Hamiltonian of an atom in the absence of radiation and term $\hbar\hat{V}$ describes the interaction of the atom with the optical and microwave fields. Let us assume that the optical field is in resonance with the transition $|F_g = 2\rangle \longleftrightarrow |F_e\rangle$ and the microwave field, with the transition $|F_g = 1\rangle \longleftrightarrow |F_g = 2\rangle$. Then, operator $\hat{V}$ has the form

$$\hat{V} = |e\rangle V_{eg_2} \exp[i(\mathbf{k} \cdot \mathbf{r} - \omega t)]\langle g_2| + |g_2\rangle U^0_{g_1 g_2}$$
$$\times \exp[i(\mathbf{q} \cdot \mathbf{r} - \omega_m t)]\langle g_1| + \text{h.c.}, \qquad (5)$$

where $V^0_{eg_2}$ and $U^0_{g_1 g_2}$ are the Rabi frequencies of the optical and microwave fields, respectively, and "h.c." means the harmonic conjugate.

Consider now matrix elements $\Gamma_{ij, kl}$ of relaxation operator $\hat{\hat{\Gamma}}$ entering into Eq. (3). Elements $\Gamma_{ee, ee} = -\gamma \approx -3.5 \times 10^7$ s^{-1} determine the rate of relaxation of the excited level populations by means of spontaneous decay. Changing the populations to the ground state via spontaneous decay is described by elements $\Gamma_{ee, ee} = \gamma P_{ge}$, where

$$P_{ge} = (2F_g + 1)(2J_e + 1)\left(C^{F_e m_e}_{F_g m_g 1 q} \left\{ \begin{array}{ccc} J_g & I & F_g \\ F_e & 1 & J_e \end{array} \right\} \right)^2 \qquad (6)$$

is the probability that the atom passes from level e to level g at spontaneous decay [14]. In (6), J_e and J_g are the respective momenta of the electron shell; F_e and F_g are the respective total momenta of the atom; m_e and m_g are the projections of the total momentum of the atom in states $|e\rangle$ and $|g\rangle$, respectively; $I = 3/2$ is the nucleus

momentum; $q = m_e - m_g$; $C^{F_e m_e}_{F_g m_g 1 q}$ is the Clebsch–Gordan coefficient; and the expression in braces is the $6J$ symbol.

In the absence of a buffer gas, the decay of "optical coherences" ρ_{eg} is described by elements $\Gamma_{eg, eg} = -\gamma'$, where $\gamma' = \gamma/2$ [15]. The relaxation of "microwave coherences" $\rho_{gg'}$ ($g \neq g'$), which is described by elements $\Gamma_{gg', gg'} = -\Gamma_\perp$, is due mainly to collisions between active atoms. It is proportional to their concentration, which, in turn, depends on the temperature of the cell. The depolarization of the ground state is taken into account through elements $\Gamma_{gg, g'g'} = \Gamma_\parallel \tilde{P}_{gg'}$ ($g \neq g'$) and $\Gamma_{gg, gg} = -\Gamma_\parallel$, where $\Gamma_\parallel \leq \Gamma_\perp$ is the depolarization rate and $\tilde{P}_{gg'}$ is the probability that the atom passes from level g' to level g.

It is assumed in the given case that transitions between these levels are equiprobable,

$$\tilde{P}_{gg'} = (2(F_{g_1} + F_{g_2}) + 1)^{-1}, \quad g \neq g'.$$

Passing to the rotating coordinate system and adiabatically eliminating populations ρ_{ee} of excited states and optical coherences ρ_{eg}, we arrive at a set of equations for populations ρ_{gg} and coherences $\rho_{gg'}$,

$$\dot{\rho}_{g_1 g_1'} = -i\Bigg[(\omega_{g_1 g_1'} - i\Gamma_\perp)\rho_{g_1 g_1'}$$

$$+ \sum_{g_2} (U^0_{g_1 g_2}\rho_{g_2 g_1'} - \rho_{g_1 g_2} U^0_{g_2 g_1'}) \Bigg]$$

$$+ \delta_{g_1 g_1'}\Bigg[\Gamma_\perp \rho_{g_1 g_1'} - \Gamma_\parallel \Bigg(\rho_{g_1 g_1} - \sum_{g''} \tilde{P}_{g_1 g''}\rho_{g'' g''} \Bigg)$$

$$+ \sum_{e, g_2'', g_2'''} 2 P_{g_1 e} \frac{V^0_{e g_1''} V^0_{g_1''' e}}{\gamma'} \tilde{G}_e \rho_{g_2'' g_2'''} \Bigg],$$

$$\dot{\rho}_{g_2 g_2'} = -i\Bigg[(\omega_{g_2 g_2'} - \Delta_{se}(1 - \delta_{g_2 g_2'}) - i\Gamma_\perp)\rho_{g_2 g_2'}$$

$$+ \sum_{g_1} (U^0_{g_2 g_1}\rho_{g_1 g_2'} - \rho_{g_2 g_1} U^0_{g_1 g_2'})$$

$$+ \sum_{e, g_2''} \frac{V^0_{g_2 e} V^0_{e g_2''}}{\gamma'} [\tilde{F}_e - i\tilde{G}_e]\rho_{g_2'' g_2'}$$

$$- \sum_{e, g_2''} \frac{V^0_{g_2'' e} V^0_{e g_2'}}{\gamma'} [\tilde{F}_e + i\tilde{G}_e]\rho_{g_2 g_2''} \Bigg]$$

(7)

$$+ \delta_{g_2 g_2'}\Bigg[\Gamma_\perp \rho_{g_2 g_2'} - \Gamma_\parallel \Bigg(\rho_{g_2 g_2} - \sum_{g''} \tilde{P}_{g_2 g''}\rho_{g'' g''} \Bigg)$$

$$+ \sum_{e, g_2'', g_2'''} 2 P_{g_2 e} \frac{V^0_{e g_2''} V^0_{g_2''' e}}{\gamma'} \tilde{G}_e \Bigg],$$

$$\dot{\rho}_{g_1 g_2} = -i\Bigg[(\omega_m - \Delta_{se} - \omega_{g_2 g_1} - \mathbf{q}\mathbf{v} - i\Gamma_\perp)\rho_{g_1 g_2}$$

$$+ \sum_{g_2'} U^0_{g_1 g_2'}\rho_{g_2' g_2} - \sum_{g_1'} \rho_{g_1 g_1'} U^0_{g_1' g_2}$$

$$- \sum_{e, g_2'} \frac{V^0_{g_2' e} V^0_{e g_2}}{\gamma'} [\tilde{F}_e + i\tilde{G}_e]\rho_{g_1 g_2'} \Bigg].$$

Here, ω_{ij} is the frequency of transition between levels i and j, $\mathbf{v} = \mathbf{p}/m$ is the velocity of the atom, δ_{ij} is the Kronecker delta, Δ_{se} is the shift due to atom–atom spin exchange interaction, and real coefficients $\tilde{F}_e$ and $\tilde{G}_e$ are related as

$$\tilde{G}_e + i\tilde{F}_e = \int_{-\infty}^{+\infty} \frac{\gamma' J(\omega')}{\gamma' - i(\omega' - \omega_{e g_2} + \Omega_L - \mathbf{k} \cdot \mathbf{v})} d\omega'. \quad (8)$$

In (8), $J(\omega')$ is the laser radiation spectral density normalized to unity,

$$\int_{-\infty}^{+\infty} J(\omega') d\omega' = 1.$$

In this work, we consider the steady regime; therefore, the partial time derivatives in the left-hand sides of Eqs. (7) are set equal to zero.

The Zeeman split of neighboring magnetic sublevels of a hyperfine level (e.g., $|g_2\rangle$) in the ground state equals about 0.7 MHz/G. In weak magnetic fields, which are applied in quantum discriminators of frequency standards to remove degeneracy (less than 1 G), this value is much smaller than both Doppler broadening $\Delta_D = 2\sqrt{\ln 2}\, k\mathbf{v}_T$ ($\mathbf{v}_T$ is the most probable velocity of atoms) of the optical transition and rate γ' of optical coherency decay. Therefore, the g_2 dependence of $\omega_{e g_2}$ in (8) can be ignored.

If the spectral density of laser radiation can be represented by a Lorentzian with thickness Γ_L (which corresponds to the diffusion model of phase noise [16]),

$$J(\omega') = \frac{\Gamma_L/2\pi}{(\omega - \omega')^2 + \Gamma_L^2/4}, \quad (9)$$

expression (8) simplifies to

$$\tilde{G}_e + i\tilde{F}_e = \frac{\gamma' + \Gamma_L/2}{\gamma' + \Gamma_L/2 - i(\omega + \Omega_L - \mathbf{kv})}. \quad (10)$$

If another type of noise dominates, expression (8) should be used. The populations of the excited states are given by the expressions

$$\rho_{exc} = \sum_{e, g_2'', g_2'''} 2\frac{V_{eg_2''}^0 V_{g_2'''e}^0}{\gamma\gamma'} \tilde{G}_e \rho_{g_2'' g_2'''}. \quad (11)$$

At 50°C, Doppler broadening $\delta_D = 2\sqrt{\ln 2}\, q\mathbf{v}_T$ of the transition $|F_g = 1, m\rangle \longleftrightarrow |F_g = 2, m\rangle$, equals about 8 kHz; the difference between the frequencies of the reference transitions $|F_g = 1, m = 0\rangle \longleftrightarrow |F_g = 2, m = 0\rangle$ and $|F_g = 1, m = \pm 1\rangle \longleftrightarrow |F_g = 2, m = \pm 1\rangle$ is about 70 kHz at magnetic field induction $B = 0.05$ G. Therefore, microwave-field-induced transitions from levels $|F_g = 1, m = \pm 1\rangle$ to levels $|F_g = 2, m = \pm 1\rangle$ can be ignored. It is convenient to introduce microwave field detuning Ω_m as

$$\Omega_m = \omega_m - \omega_{21}, \quad (12)$$

where $|1\rangle = |F_g = 1, m = 0\rangle$ and $|2\rangle = |F_g = 2, m = 0\rangle$.

Since the momentum of the atom is typically much larger than that of the photon and the concentration of active atoms is low (the free path length of active atoms is several hundreds of meters), the density matrix evolution operator can be considered to be local in coordinate and momentum. In our model, the translational degrees of freedom obey the equilibrium distribution, which yields the normalization condition in the form

$$\sum_i \rho_{ii}(\mathbf{r}, \mathbf{p}, t) = \frac{M(\mathbf{p})}{V_{cell}},$$

where

$$M(\mathbf{p}) = \frac{\exp(-p^2/p_T^2)}{(p_T\sqrt{\pi})^3} \quad (13)$$

is the Maxwell distribution function, $p_T = \sqrt{2k_B mT}$, k_B is the Boltzmann constant, and V_{cell} is the volume of the cell.

The assumptions made in our model are the following. First, atoms reflect from the walls specularly; that is, momenta $\mathbf{p}$ and $\mathbf{p}'$ of atoms before and after collision with the wall are related as $\mathbf{p}' = \mathbf{p} - 2\mathbf{n}(\mathbf{n} \cdot \mathbf{p})$, where $\mathbf{n}$ is the unit vector of the normal to surface S of the cell. Second, atomic polarization does not depend on the velocity with which the atom collides with the wall. Third, in collisions causing depolarization, transitions between sublevels of the ground state are equiprobable.

Then, for elements of the density matrix, we can write boundary conditions in the form

$$\bar{\rho}_{gg}(\mathbf{p}') - \rho_{gg}(\mathbf{r}, \mathbf{p}')_{r \in S} = \beta(\bar{\rho}_{gg}(\mathbf{p}) - \rho_{gg}(\mathbf{r}, \mathbf{p})_{r \in S}),$$

$$\rho_{gg'}(\mathbf{r}, \mathbf{p}')_{r \in S} = \alpha\rho_{gg'}(\mathbf{r}, \mathbf{p})_{r \in S}, \quad g \neq g'. \quad (14)$$

Here, $\bar{\rho}_{gg}(\mathbf{p}) = M(\mathbf{p})/8V_{cell}$ is the diagonal element of the density matrix that corresponds to complete depolarization of atoms. Coefficients α and β ($0 \leq \alpha, \beta \leq 1$) characterize the degree of relaxation of populations ρ_{gg} and coherences $\rho_{gg'}$ upon atom–wall collision.

If the interior of the cell is covered by an antirelaxation coating (such as long-chain paraffins), atoms are weakly adsorbed on the walls and the phase dispersion is also small. A large number of collisions are necessary to completely depolarize the atom. Specular coherent boundary conditions of type [13]

$$\alpha = \beta = 1 \quad (15)$$

are an idealization of such a situation.

In another extreme case, each collision of an active atom with the wall causes the complete disorientation of spin. Such a situation is typical of glass cells with alkaline element vapor and is due to a considerable spread of the magnetic field. In cells made of pyrex glass, the spread of the magnetic field reaches 5 G, because pyrex contains an appreciable amount of magnetite (0.1%), which produces ferromagnetic domains. This situation is assigned the boundary conditions of *complete quenching*: complete relaxation of coherences and equalization of populations in the atomic flow from the wall [13],

$$\alpha = \beta = 0. \quad (16)$$

Solving system (7) with boundary conditions (14) in view of (8) and integrating over the volume of the cell and momenta, we find the population in the excited state,

$$\bar{\rho}_{exc} = \iint \rho_{exc}(\mathbf{r}, \mathbf{p})d\mathbf{r}d\mathbf{p}. \quad (17)$$

Laser radiation power δP absorbed in the cell is proportional to $\bar{\rho}_{exc}$ [17],

$$\delta P = \hbar\omega\gamma N\bar{\rho}_{exc}, \quad (18)$$

where N is the number of active atoms per cell.

2. ADOPTED DEFINITIONS AND ELUCIDATORY REMARKS

In this work, we consider optical pumping by π-polarized laser field at the D_1 line. By π-polarization, we mean the situation in which laser radiation is linearly polarized and propagates in the orthogonal direction and the polarization direction coincides with the direction of permanent magnetic field $\mathbf{B}$. The magnetic field strength is $B = 0.05$ G.
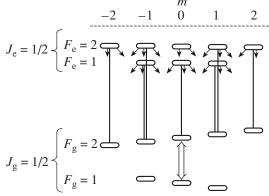
Fig. 2. DROR excitation in the ^{87}Rb atom. The microwave field acts on the reference transition $|F_g = 1, m = 0\rangle \longleftrightarrow |F_g = 2, m = 0\rangle$ (double arrow); π-polarized pumping laser field, on the transitions $|F_g = 2\rangle \longleftrightarrow |F_e\rangle$ (single arrows).

The scheme for DROR excitation is shown in Fig. 2; the geometry of such a scheme, in Fig. 3. The DROR signal, in essence, represents the dependence of current j from the detector on detuning Ω_m of the microwave field. Since the absorbed power is proportional to $\bar{\rho}_{exc}$, by the DROR signal we will mean the dependence $\bar{\rho}_{exc}(\Omega_m)$.

Let us define first the main parameters of the resonance, namely, its amplitude, width, and contrast [18]. The *amplitude* of the resonance signal is defined as the difference $\bar{\rho}_{exc}^{NR} - \bar{\rho}_{exc}^{R}$, where $\bar{\rho}_{exc}^{NR}$ is the population under no-resonance conditions and $\bar{\rho}_{exc}^{R}$ is the population under resonance. The FWHM of the DROR signal is designated as Γ_{DROR}, and the *contrast* is defined as the ratio

$$C(\Omega_m) = \frac{\bar{\rho}_{exc}(\Omega_m) - \bar{\rho}_{exc}^{NR}}{\bar{\rho}_{exc}(\Omega_m)},$$

which is convenient for DROR signal graphical representation.

We will consider the case when the optical field is in resonance with the transition $|F_g = 2\rangle \longleftrightarrow |F_e = 1\rangle$. Since in this case the hyperfine sublevels of the ground state are 817 MHz apart and the Doppler broadening of the optical transition is $\Delta_D \approx 500$ MHz, optical-field-induced transitions $|F_g = 2\rangle \longleftrightarrow |F_e = 2\rangle$ are also taken in consideration. The microwave radiation acts on the reference transition $|F_g = 1, m = 0\rangle \longleftrightarrow |F_g = 2, m = 0\rangle$. We study the shape of DROR signals for two laser radiations differing by width Γ_L of the spectrum: $\Gamma_L \approx \Delta_D$ and $\Gamma_L \leq \gamma$. The laser with $\Gamma_L \approx \Delta_D$ will be called the "wide" laser; that with $\Gamma_L \leq \gamma$, the "narrow" laser.

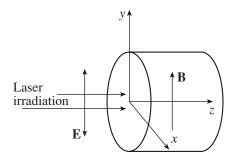Consider now the results of numerical simulation of DROR for two types of boundary conditions.

Fig. 3. Configuration providing pumping by π-polarized laser field.

3. RESULTS OF NUMERICAL CALCULATION

3.1. Specular Coherent Boundary Conditions

The results of DROR numerical simulation for specular coherent boundary conditions are presented in Fig. 4. Consider first the case of the wide laser (Fig. 4a). The effect of Dicke narrowing [19] on the DROR line shape is seen from comparison of curves *3* and *2* for cell length $a = \lambda/4$ and $3\lambda/4$, respectively. When the length of the cell is $a \geq \lambda$, one can observe the influence of radioinduced transport (RIT) of pure and mixed quantum states on the DROR line shape (curve *1*). This
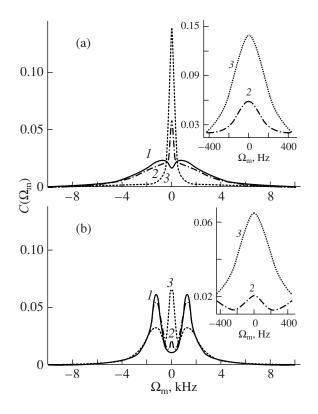

Fig. 4. DROR line shape under specular coherent boundary conditions for cell length a = (*1*) λ, (*2*) $3\lambda/4$, and (*3*) $\lambda/4$ in the case of the (a) wide and (b) narrow laser. $\Gamma_\perp = 100$ s^{-1}, $U^0 = 300$ s^{-1}, and $I = 20$ μW/cm^2. The inset shows the DROR line shape in a narrower range of Ω_m.

effect was first considered in terms of a three-level model [13, 20, 21].

The physical reason for the RIT effect is the Doppler-induced velocity selectivity of interaction between the microwave field and active atoms. It gives rise to Bennett dips and peaks [22] in the velocity distributions of atoms in long-lived states $|1\rangle$ and $|2\rangle$, the transition between which interacts with the microwave field.

Skewness of the velocity distribution causes counterflows of atoms in these states along the direction of microwave propagation. In this case, one can speak of inversion flux and population freezing-out (for details, see [21]).

Consider now the case in which the narrow laser is used for optical pumping. It follows from Fig. 4b (curves *3* and *2* for $a = \lambda/4$ and $3\lambda/4$, respectively) that, first, the Dicke effect influences the DROR line shape at $a \leq \lambda$, as in the case of the wide laser. However, the DROR contrast is roughly twice as weak as in the case of the wide laser, since here only atoms with a certain velocity contribute to the resonance.

The other feature related to the narrow laser is the effect of laser-induced transport (LIT) of quantum states [23, 24], which takes place at $a \geq \lambda/8$ and influences the DROR line shape.
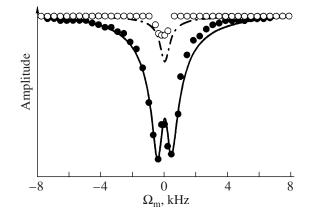
The LIT effect shows up similarly to the RIT effect: fluxes of atoms in different long-lived states arise. However, in the former case, Bennett dips and peaks (and hence the velocity skew distribution) are related to the use of the narrow laser. Note that the LIT effect is observed in both the standing and traveling microwave unlike the RIT effect, which can be observed only in a traveling microwave.

The RIT effect, as well as the LIT effect, plays a prominent (and sometimes decisive) role in DROR formation. However, these effects are absent when the cell is shorter than $\lambda/8$. In this work, we consider a one-dimensional model of the flat layer. In real (three-dimensional) cells, the side walls (as well as the frequency modulation of the microwave field) tend to quench both RIT and LIT, which makes them difficult to observe.

In [1, 12, 25], the influence of LIT on the DROR line shape was not observed because of the three-dimensional motion of atoms and weak microwave and optical fields. In [26], where the DROR was studied in strong fields, the influence of LIT was noticeable. Interestingly, this effect was observed in a glass (without a wall antirelaxation coating) cell. Such a situation will be discussed below.

However, the results concerning the Dicke effect remain valid for the 3D motion of atoms as well. A relevant analysis was carried out in [27]. Its basic results are given below.

In the 3D model, the free path length of atoms equals length a of the cell and the atom–wall collision frequency is $\nu = |v_z|/a$. In other words, the microwave
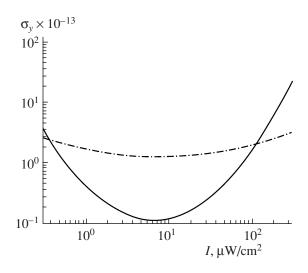

Fig. 5. DROR signal shape at different intensities of the optical field under complete quenching boundary conditions (optical pumping by the narrow laser). Circles are data points from [26] (filled and empty ones corresponds to various pumping intensities); solid lines, our calculation. Input data for calculation (Rabi frequency of the microwave field, optical field intensity, cell size, etc.) are taken from [26].

radiation is modulated with frequency ν, which gives rise to two side frequencies $\nu_{21} \pm \nu$ in addition to center frequency ν_{21}. Averaging over an atomic ensemble adds a wide pedestal to a narrow central peak. In a 3D cell with radius a, the free path length is no longer fixed and runs from 0 to a. The modulation frequency varies from ν to ∞, so that two side frequencies are replaced by two side bands. The pedestal changes form, but the narrow peak (Dicke narrowing) persists. Note that the three-dimensionality of the cell enhances the Dicke effect compared with the one-dimensional cell and the three-dimensional motion of atoms smoothes out and eventually quenches LIT and RIT.

3.2. Complete Quenching Boundary Conditions (Glass Cell)

In this case, the DROR signal is weak and cannot be detected experimentally when the intensity of the laser field and the Rabi frequencies of the microwave radiation are low (the situation considered in the previous subsection). Therefore, it is necessary to raise the Rabi frequency of the microwave field and intensity of optical pumping by several orders of magnitude to make the DROR signal observable. In [26], a dip at the DROR line center was observed when ^{85}Rb atomic vapor was placed in high fields. This finding is a direct consequence of the influence of LIT on the DROR line shape.

Our calculated results are in good qualitative agreement with experimental data derived in [26] (Fig. 5). Interestingly, there exists a critical intensity of the optical field at which the DROR signal shape changes radically and it begins to depend on the Rabi frequency of the microwave field [26].

$\sigma_y \times 10^{-13}$

Fig. 6. Short-term stability vs. laser field intensity under specular coherent boundary conditions (integration time $\tau = 1$ s). Cell length $a = 3$ cm, $\Gamma_\perp = 100$ s^{-1}, and $U^0 = 300$ s^{-1}. The solid and dash-and-dot lines correspond to the wide and narrow laser, respectively.

4. SHORT-TERM STABILITY IN THE SHOT NOISE LIMIT

Let us analyze short-term stability $\sigma(\tau)$ of a quantum discriminator of a frequency standard using a cell without an antirelaxation wall coating. This parameter is inversely proportional to figure of merit Q. In the shot noise limit, $\sigma(\tau)$ is given by [5, 17]

$$\sigma(\tau) = \frac{\sqrt{j}e}{S\tilde{\Gamma}\omega_{\text{hfs}}\sqrt{\tau}}, \tag{19}$$

where $\tilde{\Gamma}$ is the width of a linear section in the discrimination curve (a section near the resonance peak over which the second derivative of the photocurrent with respect to microwave field detuning remains almost constant); S is the steepness, which is equal to the absolute value of the second derivative with respect to detuning Ω_m in the peak of radiation absorption; e is the electron charge; ω_{hfs} is the frequency of a hyperfine transition in the ground state; and τ is the averaging time.

Figure 6 plots the short-term stability of the frequency standard in the case of DROR versus the laser field intensity. It is seen that a high stability can be obtained using the wide laser (for the narrow laser, the stability is an order of magnitude lower). An optimal value of optical radiation intensity I falls into the range 6–10 μW/cm^2. The reason for the discrepancy in the stability is that the number of atoms contributing to the DROR is much greater in the case of the wide laser.

When pumping is accomplished by the narrow laser, the stability is on the order of 10^{-13}. Our estimates of the stability confirm the data obtained in [28], where the short-term stability was found to be 2×10^{-13}. It should

be emphasized here that calculations were carried out in the shot noise limit without allowance for amplitude and electrical noise, laser frequency drift, etc.

CONCLUSIONS

We studied the formation of radiooptical resonance in ^{87}Rb atomic vapor in a cell with an antirelaxation coating. Two types of lasers were considered that differ in radiation spectrum width: wide laser ($\Gamma_L \approx \Delta_D$) and narrow laser ($\Gamma_L \leq \gamma$). It was shown that the DROR line narrows (Dicke effect) under specular coherent boundary conditions. Using a narrow laser makes it possible to observe the influence of the laser-induced transport of long-lived states on the DROR signal shape, while using a wide laser allows one to improve the short-term stability by an order of magnitude compared with the case of the narrow laser.

Although emphasis in this work is on designing precision quantum frequency standards, the results will be useful in designing precision magnetometers.

REFERENCES

1. D. Budker, L. Hollberg, D. F. Kimball, et al., Phys. Rev. A **71**, 012903 (2005).
2. M. V. Balabas, D. Budker, J. Kithing, et al., J. Opt. Soc. Am. B **23**, 1001 (2006).
3. E. Hodby, E. A. Donley, and J. Kitching, Appl. Phys. Lett. **91**, 011109 (2007).
4. S. Knappe, P. D. D. Schwindt, V. Gerginov, et al., J. Opt. A: Pure Appl. Opt. **8**, 318 (2006).
5. J. Vanier and C. Audoin, *The Quantum Physics of Atomic Frequency Standarts* (Higler, Bristol, 1989).
6. N. M. Pomerantsev, V. M. Ryzhkov, and G. V. Skrotskii, *Physical Basis of Quantum Magnetometry* (Nauka, Moscow, 1972) [in Russian].
7. V. Shahl, S. Knappe, P. D. D. Schwindt, et al., Nature Photonics **1**, 649 (2007).
8. D. Budker and M. Romalis, Nature Phys. **3**, 227 (2007).
9. M. H. Acuna, *Encyclopedia of Planetary Sciences,* Ed. by J. H. Shirley and R. W. Fairbridge (Chapman, London, 1997), pp. 406–410.
10. H. Robinson, E. Ensberg, and H. T. Dehmelt, Bull. Am. Phys. Soc. **3**, 9 (1958).
11. M. T. Graf, D. F. Kimball, S. M. Rochester, et al., Phys. Rev. A **72**, 023401 (2005).
12. J. S. Guzman, A. Wojciechowski, J. E. Stalnaker, et al., Phys. Rev. A **74**, 053415 (2006).
13. B. D. Agap'ev, M. B. Gornyi, and B. G. Matisov, Zh. Tekh. Fiz. **58**, 2286 (1988) [Sov. Phys. Tech. Phys. **33**, 1394 (1988)].

14. D. A. Varshalovich, A. N. Moskalev, and V. K. Kherson-skii, *Quantum Theory of Angular Momentum* (Nauka, Leningrad, 1975; World Sci., Singapore, 1988).

15. G. A. Kazakov, B. G. Matisov, I. E. Mazets, and Yu. V. Rozhdestvensky, Zh. Tekh. Fiz. **76** (4), 20 (2006) [Tech. Phys. **51**, 1414 (2006)].

16. I. E. Mazets and B. G. Matisov, Zh. Éksp. Teor. Fiz. **101**, 26 (1992) [Sov. Phys. JETP **74**, 13 (1992)].

17. M. B. Gornyi, B. G. Matisov, G. M. Smirnova, et al., Zh. Tekh. Fiz. **57**, 740 (1987) [Sov. Phys. Tech. Phys. **32**, 448 (1987)].

18. G. Kazakov, B. Matisov, I. Mazets, et al., Phys. Rev. A **72**, 063408 (2005).

19. R. H. Dicke, Phys. Rev. **89**, 472 (1953).

20. B. D. Agap'ev and B. G. Matisov, Pis'ma Zh. Tekh. Fiz. **12**, 123 (1986) [Sov. Tech. Phys. Lett. **12**, 51 (1986)].

21. B. D. Agap'ev and B. G. Matisov, Pis'ma Zh. Éksp. Teor. Fiz. **44**, 66 (1986) [JETP Lett. **44**, 81 (1986)].

22. W. R. Bennett, Phys. Rev. **126**, 580 (1962).

23. B. D. Agap'ev, M. B. Gornyi, and B. G. Matisov, Opt. Spektrosk. **61**, 1155 (1986) [Opt. Spectrosc. **61**, 723 (1986)].

24. B. D. Agap'ev, M. B. Gornyi, and B. G. Matisov, Zh. Éksp. Teor. Fiz. **92**, 1995 (1987) [Sov. Phys. JETP **67**, 1121 (1987)].

25. M. Klein, I. Novikova, D. F. Phillips, et al., J. Mod. Opt. **53**, 2583 (2006).

26. A. S. Zibrov, A. S. Zhukov, V. P. Yakovlev, and V. L. Veli-chansky, Pis'ma Zh. Éksp. Teor. Fiz. **83**, 168 (2006) [JETP Lett. **83**, 136 (2006)].

27. R. P. Frueholz and C. H. Volk, J. Phys. B **18**, 4055 (1985).

28. C. Szekely, R. E. Drullinger, F. L. Walls, et al., in *Proc. IEEE Int. Frequency Control Symp., 1993,* pp. 41 518–41 521.